Scientia Iranica A (2013) 20(4), 1161–1174

Sharif University of Technology
Scientia Iranica
Transactions A: Civil Engineering
www.scientiairanica.com

Updated Lagrangian large deformation analysis of consolidation settlement with finite element method for a case study in Iran

M. Veiskarami*

Department of Civil Engineering, Faculty of Engineering, University of Guilan, Iran.

Received 11 September 2012; received in revised form 14 December 2012; accepted 5 February 2013

KEYWORDS
Consolidation;
Large strain;
Updated Lagrangian formulation;
Finite element;
Settlement.

Abstract. Settlement of fine-grained soils is often governed by a consolidation process which involves quite large strains. The classic, one-dimensional consolidation formula is based on the small strain theory, although it is still practically useful. Since strains are relatively large during the consolidation process, the overall behavior of the medium is geometrically nonlinear. In this paper, a coupled consolidation analysis was carried out to predict the consolidation settlement of ground beneath an embankment, as a case study, representing the feasibility of large strain consolidation analysis. A two-dimensional, updated Lagrangian, large deformation, finite element formulation was employed to simultaneously solve the transient flow and the deformation equations which constitute the coupled consolidation equations. It was followed by the development of a code in the MATLAB environment to solve the required equations, with further application to a case study in Iran. In addition, analyses were performed by one-dimensional conventional methods and compared with the results obtained by the finite element procedure. Predictions made by large deformation finite element analysis, in comparison to those obtained based on small strain assumptions and conventional methods, appeared to be more accurate, although the required computational effort was much higher, owing to frequent recomputation of the stiffness matrix.

1. Introduction

The theory of consolidation, dating back to the renowned, one-dimensional consolidation theory of Terzaghi (1943) [1], has been subjected to several changes and considerable developments. The consolidation process refers to the entire process of time-dependent deformation of soil due to drainage and gradual dissipation of excess pore water pressure. Therefore, the transient flow and deformation equations are both necessary to formulate the consolidation process [1-3]. In the original theory, there are several simplifying assumptions, which can only be satisfied under particular conditions and in very rare problems. Among many, the strains were assumed to be small, and the compressibility and hydraulic conductivity were combined into a unique and constant coefficient, known as the coefficient of consolidation. There are two common forms of (uncoupled) consolidation equation; the first, derived by Terzaghi (1943), is [1]:

$$\frac{\partial U}{\partial t} = C_v \frac{\partial^2 U}{\partial z^2}. \tag{1}$$

In this equation, U is the excess pore water pressure, t is the time, z is a measure of distance (often vertical) and C_v is the coefficient of consolidation (often in a vertical direction). This equation is analogous to the

*. *Email addresses: mveiskarami@gmail.com and mveiskarami@shirazu.ac.ir*

heat transfer equation and can be extended to two or three dimensions, as follows, assuming the coefficient of consolidation is constant in all directions:

$$\frac{\partial U}{\partial t} = C_v \nabla^2 U. \tag{2}$$

The second common form, in terms of strain, was suggested by Mikasa (1963), as follows [4]:

$$\frac{\partial \varepsilon_z}{\partial t} = C_v \frac{\partial^2 \varepsilon_z}{\partial z^2}, \tag{3}$$

where ε_z is the linear strain in the vertical direction. It can be seen that both equations are similar in form, possessing the coefficient of consolidation, defined as follows:

$$C_v = \frac{k}{m_v \gamma_w}. \tag{4}$$

In this equation, k is the coefficient of hydraulic conductivity, γ_w is the unit weight of pore fluid (often water) and m_v is the volume compressibility coefficient of the soil skeleton.

There may have been several questions regarding the validity of such assumptions, motivating the authors to develop the theory of consolidation. For example, assuming a constant parameter, m_v, for the entire range of applied loads, may be somehow unrealistic, regarding the nonlinear response of fine soils to the applied loads. It works almost well only in the range of small strains and light loads. For heavy loads, it can no longer be regarded as a true assumption, leading to less accurate predictions.

Known to the author, several attempts have been made in the development of the consolidation theory to consider the nonlinearity of the consolidation settlement by taking several assumptions into account. Among many, Gibson et al. (1967) and Gibson et al. (1981) developed the theory of finite strain, one-dimensional consolidation for thin (in 1967) and thick (in 1981) layers of soft soil [5,6]. It was a very successful attempt since it did not rely upon small strains and other restrictive assumptions. However, it requires complicated laboratory test results to find proper relations between soil mechanical parameters (such as hydraulic conductivity, etc.) based on primary ones (like void ratio and pressure). The derived differential equation is also highly nonlinear. Huerta and Rodriguez (1992) presented a finite difference based numerical scheme to solve this equation by assuming the excess pore water pressure to be the dependent variable [7]. They first cast the equation in a non-dimensional form and then constituted a fully implicit finite difference nonlinear matrix equation, which showed a relatively rapid and stable convergence.

Applications of the finite element method in solving one and multi dimensional consolidation equations are many. For example, Desai and Johnson (1972) compared two finite element methods for the one-dimensional consolidation equation [8]. Johnson (1978) presented a coupled finite element method to solve the flow and small strain deformation equations [9]. He proved that a solution existed for an elasto-plastic constitutive model, and presented the finite element formulation of the equation. Duncan and Schaefer (1988) applied the finite element method to analyze the consolidation of embankments with the Cam Clay constitutive model [10]. Borja et al. (1998) employed hypo-elasticity and developed an elasto-plastic consolidation analysis by a nonlinear finite element method [11]. Their attempt was very important since it presents the effect of geometrical nonlinearity on the results. Kelln et al. (2009) applied the finite element method in consolidation analysis of a soft estuarine soil by implementation of an elastic-viscoplastic model [12]. In 2010, Huang and Griffiths presented a finite element method for both coupled and uncoupled one-dimensional consolidation analysis of a multilayer soil [13]. Very recently, Samimi and Pak (2012) presented a fully coupled three-dimensional analysis of porous continua containing solid particles and pore fluids with the element free Galerkin method [14].

The nonlinear behavior of soil during the consolidation process has been generally accepted in these attempts, and the source of nonlinearity is often attributed to the nonlinear behavior of the material. In contrast, relatively little attention has been paid to the nonlinear behavior, due to the geometrical nonlinearity originated from large deformations. In fact, there are two sources for a nonlinear response in deforming bodies, i.e. material nonlinearity and geometrical nonlinearity [15,16]. Material nonlinearity can be taken into account by relatively complicated elasto-plastic soil models (as in the consolidation analysis, amongst a few found in the literature, the important works of Borja and Alarcón in 1995 and Borja et al. in 1998, or, more recently, Kelln et al. (2009) [11,12,17] should be mentioned), whereas geometrical nonlinearity must be tackled by the theory of finite strain. In this paper, the consolidation process has been analyzed by both small and large strain formulations. The pore fluid flow equation, along with the deformation equations, has been coupled in a finite element code by the updated Lagrangian large deformation formulation. First, the theoretical requirements and equations have been represented. Then, the developed finite element code is applied to a case study, where a medium clay stratum underlain by a stiff to hard clay is subjected to preloading under the pressure of a massive embankment.

2. Behind the theory

As stated earlier, the one-dimensional consolidation equations of Terzaghi (1943) [1] or Mikasa (1963) [4], which are equivalent, have been developed for certain and partly idealized soil conditions. Moreover, these equations were derived for the case of one-dimensional deformation of the soil. In two or three dimensions, however, there are several complexities in finding a solution to these equations, in particular, in complex domains and under general initial conditions. These equations, in fact, can be classified into standard partial differential equations in mathematical physics, with known solutions in the simple domain, in which they are subjected to standard initial and boundary conditions. The finite element method has been found to be a powerful technique for solving the consolidation equation, in particular for cases with certain difficulties, like multilayer soils, non-homogeneous soils and for two and three dimensional problems. In multidimensional problems, the coupled consolidation equations comprise a set of pore fluid flow equations which governs the flow of pore fluid passing through the soil body and the deformation equation. The system of equations governs the simultaneous deformation of the consolidating body, while the drainage of the pore fluid takes place and the space initially occupied by the pore fluid is replaced by solid particles. During this process, if strains are assumed to be small, the stress-strain behavior of the solid phase, i.e. the soil skeleton, can be regarded as linear. Therefore, the load-displacement behavior of the material will be linear as well. However, for a relatively large deformation, which is the case in settlement analysis, in spite of a possible linear stress-strain relationship, which is practically assumed, based on standard laboratory tests, by simply taking a constant parameter, m_v, the load-deformation response is not linear. Such nonlinearity, known as geometrical nonlinearity, can be regarded as a source of nonlinear response. This latter can be taken into account in the consolidation analysis, where soil properties obtained by routine and standard laboratory tests are sufficient to perform a more accurate analysis. In the next part, application of geometrical nonlinearity and further assumptions are presented. This scheme seems to be convenient, since it depends solely on conventional (standard) laboratory soil tests and not on more sophisticated elasto-plastic soil models. Although the change in soil permeability and deformability during the consolidation process is important, requiring a more precise consideration of the chosen constitutive law, as both permeability and deformability decrease over the course of the consolidation process, their ratios may be subject to an insignificant change. They can be, therefore, *assumed* to remain constant, and the nonlinear response to be related only to geometrical (large strain) nonlinearity.

3. Coupled consolidation with large strain analysis

All required governing equations to be solved in a coupled transient flow-deformation analysis are presented here. These equations can be found in more detail in advanced texts (e.g. [15-21]). It is worth mentioning that in all equations, the following notations are used, which are used by Reddy (2004) [19]. In an incremental procedure, it is assumed that a deforming body, initially at C_0 configuration, deforms from C_1 configuration to C_2 configuration, and an increment of deformation between these two last configurations takes place. In all quantities, a left subscript is used to denote the configuration, with respect to which, the quantity is measured, whereas a left superscript refers to the configuration in which the quantity has already occurred. Between two successive configurations, C_1 and C_2, the left superscript may be skipped over, indicating an increment of the quantity under consideration. Other notations are standard notations used in tensor algebra and continuum mechanics [15,19,21].

The first required equation in time-dependent consolidation is the static equilibrium equation:

$$\boldsymbol{\nabla}.\boldsymbol{\sigma} + \underline{\mathbf{b}} = \frac{\partial \sigma_{ji}}{\partial x_j} + b_i = 0, \tag{5}$$

where $\boldsymbol{\sigma}$ is the matrix of Cauchy stresses, $\mathbf{b}$ is the vector of body and/or inertial forces, $\sigma_{ji,j}$ are components of partial derivatives of the stress tensor, σ_{ij}, and b_i are components of body and/or inertial forces. The continuity (flow) equation, assuming Darcy's law to be valid, is as follows:

$$\frac{k}{\gamma_w}\nabla^2 U + Q = m_v \frac{\partial U}{\partial t}. \tag{6}$$

In this equation, k is the soil permeability coefficient, γ_w is the unit weight of the pore fluid, Q represents a sink or a source for the pore fluid dissipation or generation, and other terms were defined earlier.

In small deformation analysis, stresses are related to the strains through a general constitutive law:

$$\boldsymbol{\sigma} = \mathbf{D} : \mathbf{e}, \tag{7}$$

$$\sigma_{ij} = D_{ijkl} e_{kl}. \tag{8}$$

In this equation, $\mathbf{D}$ (or D_{ijkl}) is the fourth-order constitutive tensor and $\mathbf{e}$ (or e_{kl}) is the Cauchy strain tensor. The Cauchy (infinitesimal) strain tensor is defined as:

$$e_{kl} = \frac{1}{2}\left(\frac{\partial u_k}{\partial x_l} + \frac{\partial u_l}{\partial x_k}\right), \tag{9}$$

where u_k and u_l are components of displacements in k and l directions, respectively. In an updated Lagrangian analysis, a constitutive equation of the following form will be required:

$$_1S_{ij} = {_1D_{ijkl}} {^2_1\varepsilon_{kl}}, \tag{10}$$

where $_1S_{ij}$ is the updated Kirchhoff stress increment tensor, $_1D_{ijkl}$ is the constitutive tensor and $_1\varepsilon_{kl}$ is the updated Green-Lagrange strain increment tensor. It is conventional to adopt a constant incremental constitutive tensor (i.e. assuming $_0D_{ijkl} = {_1D_{ijkl}}$) in different configurations in an updated (and even total) Lagrangian formulation [19]. In the updated Lagrangian formulation, the following relationships and approximations are used:

$$^1_1\varepsilon_{kl} = \frac{1}{2}\left(\frac{\partial\, ^1_0u_k}{\partial\, ^1x_l} + \frac{\partial\, ^1_0u_l}{\partial\, ^1x_k} - \frac{\partial\, ^1_0u_m}{\partial\, ^1x_k}\frac{\partial\, ^1_0u_m}{\partial\, ^1x_l}\right), \tag{11}$$

$$\begin{aligned} ^2_1\varepsilon_{kl} &= \frac{1}{2}\left(\frac{\partial u_k}{\partial\, ^1x_l} + \frac{\partial u_l}{\partial\, ^1x_k} + \frac{\partial u_m}{\partial\, ^1x_k}\frac{\partial u_m}{\partial\, ^1x_l}\right) \\ &= \frac{1}{2}\left({_1e_{kl}} + {_1\eta_{kl}}\right), \end{aligned} \tag{12}$$

$$_1e_{kl} = \frac{1}{2}\left(\frac{\partial u_k}{\partial\, ^1x_l} + \frac{\partial u_l}{\partial\, ^1x_k}\right), \tag{13}$$

$$_1\eta_{kl} = \frac{1}{2}\left(\frac{\partial u_m}{\partial\, ^1x_k}\frac{\partial u_m}{\partial\, ^1x_l}\right), \tag{14}$$

$$^2_1S_{ij} = {^1\sigma_{ij}} + {_1S_{ij}}, \tag{15}$$

$$^1_1S_{ij} = {^1\sigma_{ij}}, \tag{16}$$

$$^1\sigma_{ij} = {_1D_{ijkl}} {^1_1\varepsilon_{kl}}, \tag{17}$$

$$_1S_{ij} = {_1D_{ijkl}} {^2_1\varepsilon_{kl}} \approx {_1D_{ijkl}} {_1e_{kl}}. \tag{18}$$

In these equations, $^1_1\varepsilon_{kl}$ is the Almansi-Hamel strain tensor (also known as the Euler strain tensor) which appears naturally in the updated Lagrangian formulation, $^2_1\varepsilon_{kl}$ is the updated Green-Lagrange strain tensor, $^1_0u_k$ are components of displacement, which occur at C_1 configuration, measured in C_0 configuration, ^1x_l are coordinates of the system in C_1 configuration, $^1e_{kl}$ is the linear part of the strain increment tensor, $^1\eta_{kl}$ is the nonlinear part of the strain increment tensor, $^2_1S_{ij}$ are components of the updated Kirchhoff stress tensor, $^1\sigma_{ij}$ are components of the Cauchy stress tensor in C_1 configuration and $_1S_{ij}$ are components of the updated Kirchhoff stress tensor increment. It is remarkable that the latter simplification (resulting in a symmetric term in computation of the stiffness matrix) is valid only if the incremental deformations (and hence, strains) are reasonably small. Having known all these quantities, the principle of virtual work can now be applied to find the required finite element formulation of the deformation problem:

$$\delta W_{\text{int}} = \delta W_{\text{ext}}, \tag{19}$$

where, δW_{int} is the internal virtual energy increment and δW_{ext} is the external virtual work increment, which are defined as follows:

$$\delta W_{\text{int}} = \int_{^1V} {^2_1S_{ij}}\,\delta\, {^2_1\varepsilon_{ij}}\,dV, \tag{20}$$

$$\delta W_{\text{ext}} = \delta\, {^2_1R} = \int_{^1A} {^2_1t_i}\,\delta u_i\,dA + \int_{^1V} {^2_1b_i}\,\delta u_i\,dV. \tag{21}$$

In these equations, $^2_1t_i$ are components of the traction forces and $^2_1b_i$ are components of body forces. By equating the external virtual work increment with the internal virtual energy increment and after some manipulations and substitution of the abovementioned equations, the weak form of the governing equation required for the updated Lagrangian finite element formulation will be found as follows:

$$\begin{aligned} &\int_{^1V} {_1D_{ijkl}}\ {_1e_{kl}}\,\delta\ {_1e_{ij}}\,dV + \int_{^1V} {^1\sigma_{ij}}\,\delta\ {_1\eta_{ij}}\,dV \\ &\qquad = \delta {^2_1R} - \int_{^1V} {^1\sigma_{ij}}\,\delta\ {_1e_{ij}}\,dV. \end{aligned} \tag{22}$$

Finally, by applying the lemma of calculus of variations, the system equations of the updated Lagrangian finite element formulation are as follows [19]:

$$(\mathbf{K_L} + \mathbf{K_{NL}})\boldsymbol{\Delta}\underline{\mathbf{u}} = {^\mathbf{2}_\mathbf{1}\underline{\mathbf{F}}} - {^\mathbf{1}_\mathbf{1}\underline{\mathbf{F}}}, \tag{23}$$

where $\mathbf{K_L}$ and $\mathbf{K_{NL}}$ are contributing parts of the stiffness matrix, $\boldsymbol{\Delta}\underline{\mathbf{u}}$ is the nodal displacement increment vector (defined between two successive steps), and $^\mathbf{2}_\mathbf{1}\underline{\mathbf{F}}$ and $^\mathbf{1}_\mathbf{1}\underline{\mathbf{F}}$ are vectors of nodal forces in two successive steps. These quantities are defined as follows:

$$\mathbf{K_L} = \int_{^0V} \mathbf{B_L^T D B_L}\,dV, \tag{24}$$

$$\mathbf{K_{NL}} = \int_{^1V} \mathbf{B_{NL}^T}\ {^\mathbf{1}\boldsymbol{\sigma}}\mathbf{B_{NL}}\,dV, \tag{25}$$

$$^\mathbf{2}_\mathbf{1}\underline{\mathbf{F}} = \int_{^1V} \boldsymbol{\Phi}^\mathbf{T}\, {^\mathbf{2}_\mathbf{1}\underline{\mathbf{b}}}\,dV + \int_{^1A} \boldsymbol{\Phi}^\mathbf{T}\, {^\mathbf{2}_\mathbf{1}\underline{\mathbf{t}}}\,dA, \tag{26}$$

$$^\mathbf{1}_\mathbf{1}\underline{\mathbf{F}} = \int_{^1V} \mathbf{B_L^T}\, {^\mathbf{1}\underline{\boldsymbol{\sigma}}}\,dV. \tag{27}$$

In these equations, $\boldsymbol{\Phi}$ is the matrix containing the element interpolation functions, $\underline{\mathbf{b}}$ is the vector of body and/or inertial forces, $^\mathbf{1}\boldsymbol{\sigma}$ is the matrix of the Cauchy stresses, ${}^{1}\underline{\boldsymbol{\sigma}}$ is the vector containing the stress components and $\underline{\mathbf{t}}$ is the vector of surface tractions (note that the under bar sign denotes a vector quantity). The other quantities are presented in Appendix A of this paper.

Now, by dividing the total stress into the effective stress and the pore water pressure, the abovementioned equation can be cast into the following one required for the consolidation analysis:

$$(\mathbf{K_L} + \mathbf{K_{NL}})\boldsymbol{\Delta}\underline{\mathbf{u}} + \mathbf{L}\boldsymbol{\Delta}\mathbf{U_N} = {}^{2}_{1}\underline{\mathbf{F}} - {}^{1}_{1}\underline{\mathbf{F}}. \tag{28}$$

The additional term, i.e. $\mathbf{L}\boldsymbol{\Delta}\mathbf{U_N}$, is responsible for the excess pore water pressure developed through the element, and $\mathbf{L}$ is the coupling matrix giving rise to the nodal forces due to the excess pore water pressure build up, defined as follows:

$$\mathbf{L} = \int_{{}^{1}V} \mathbf{B_L^T}\mathbf{m}\underline{\boldsymbol{\Phi}}dV, \tag{29}$$

where $\mathbf{m} = \begin{bmatrix}1 & 1 & 0\end{bmatrix}^T$ for two-dimensional problems and $\underline{\boldsymbol{\Phi}}$ is a vector containing the element interpolation function.

In addition to the deformation formulation, the transient flow problem required for the coupled analysis can be formulated by the finite element procedure. Substitution of Darcy's law and applying the Galerkin finite element method results in the following equation:

$$-\mathbf{H}\boldsymbol{\Delta}t + \mathbf{L^T}\boldsymbol{\Delta}\underline{\mathbf{u}} = \underline{\mathbf{q}}\boldsymbol{\Delta}t, \tag{30}$$

where $\mathbf{H}$ is the element conductance matrix, $\underline{\mathbf{q}}$ is the nodal flow vector and Δt is the time increment. The element conductance matrix can be computed as follows:

$$\mathbf{H} = \frac{1}{\gamma_w}\int_{{}^{1}V} (\nabla\boldsymbol{\Phi})^{\mathbf{T}}\mathbf{R}\boldsymbol{\nabla}\boldsymbol{\Phi}dV. \tag{31}$$

In this equation, $\mathbf{R}$ is the matrix of the element conductivity coefficients defined (in two dimensional problems) as follows:

$$\mathbf{R} = \begin{bmatrix}k_x & 0\\ 0 & k_y\end{bmatrix}. \tag{32}$$

Eventually, the coupled consolidation equation can be found by a combination of the deformation and flow equations:

$$\begin{bmatrix}\mathbf{K} & \mathbf{L}\\ \mathbf{L^T} & -\alpha\Delta t\mathbf{H}\end{bmatrix}\begin{bmatrix}\boldsymbol{\Delta}\underline{\mathbf{u}}\\ \boldsymbol{\Delta}\mathbf{U_N}\end{bmatrix} = \begin{bmatrix}\mathbf{0} & \mathbf{0}\\ \mathbf{0} & -\Delta t\mathbf{H}\end{bmatrix}\begin{bmatrix}{}^{1}\underline{\mathbf{u}}\\ {}^{1}\mathbf{U_N}\end{bmatrix} + \begin{bmatrix}{}^{2}_{1}\underline{\mathbf{F}} - {}^{1}_{1}\underline{\mathbf{F}}\\ \Delta t({}^{1}\underline{\mathbf{q}} + \alpha\Delta{}^{1}\underline{\mathbf{q}})\end{bmatrix}. \tag{33}$$

This is the final form of the finite element equation of the coupled consolidation problem by the updated Lagrangian large deformation formulation. The coefficient, α, takes values ranging from 0 to 1. For a fully implicit integration, this value is set equal to 1. There are restrictions on the time step in the marching procedure in solving the system of the coupled equations in order to arrive at a stable solution. For example, α cannot take values less than 0.5 [22]. A similar approach can be used to formulate the coupled consolidation problem with the small strain assumption, where the element stiffness matrix and the coupled matrix are not updated during each displacement increment.

The finite element formulation developed so far has been implemented in the MATLAB environment and used for the rest of this study. Through all analyses, the following assumptions were made:

i) The same interpolation functions have been used in computing stiffness, coupling and conductance matrices.

ii) The initial distribution of the excess pore water pressure is computed by assuming a Poisson ratio equal to 0.49, but this ratio was taken equal to 0.35 for the rest of the computations.

iii) The constitutive tensor was assumed to be the same for both small strain and large strain analyses.

4. Case study: A preloaded area in the northern Iran

As stated earlier, the nonlinear behavior of soil, when subjected to external loads leading to a consolidation process, can be captured in a more realistic way when a large deformation analysis is carried out. A case study is presented here, in which, the large deformation theory has been employed to predict the settlements due to a staged preloading. In order to prepare a site to support heavy loads of large storage tanks, it was preloaded for a rather long time. The site was located in north-eastern Iran, part of the Urea and Ammonia Unit Plant of the Golestan Petrochemical Company, and the soil profile mainly consisted of rather uniform and lightly overconsolidated soft to medium clay and silt down to 28 m to 32 m deep, where a relatively stiff to hard clay existed. The area under study was roughly between 32 m to 40 m wide and 75 m to 90 m long. The geotechnical consultant performed a series of consolidation tests, as well as other standard laboratory and field tests, to characterize the soil profile. Table 1 presents a summary of the required geotechnical properties obtained by site investigations and laboratory tests.

Table 1. A summary of the subsoil properties.

Properties	Range	Assumed (averaged) values
Depth (m)	0-30	-
Classification	CL/ML	-
Moisture content (%)	20-26	23
Dry unit weight (kN/m^3)	15.2-16.9	16.0
Void ratio (%)	0.57-0.74	0.6
Liquid limit (%)	27-31	29
Plasticity index (%)	9-14	12
Volume compressibility, $\mathbf{m_v}$ (m^2/kN)	6.5e-5 to 2.0e-4	1.1e-4 (average of 7 tests)
Compression index ($\mathbf{C_c}$)	0.056-0.171	0.103 (average of 7 tests)
Swelling/recompression index ($\mathbf{C_s}$)	0.007-0.034	0.011 (average of 7 tests)
OCR	1.09-1.25	1.16
Unconfined compressive strength (kPa)	25-50	38 kPa

(a) (b) (c)

Figure 1. Preloading program: (a) A side view of the preloaded area (still under construction); (b) a closer view from the east side; and (c) a schematic view of the reference bar.

Preloading was performed by the staged construction of an embankment with a total height of 8.0 m above ground level. The unit weight of the material was roughly around 15 kN/m^3 and the entire process of the embankment took 22 days. Measurements were carefully taken by installation of a reference mark (a vertical rod installed over the ground surface before the preloading started) in the centre of the embankment area. Recordings were made at the end of each working day, with respect to some stable reference point installed on stable ground far from the deforming area, by survey cameras. Figure 1 shows the almost finished embankment. In the same figure, a schematic view of the installed rod(s) is depicted with their elevations, with respect to the reference ground level.

Analyses were made first to calibrate the model for laboratory tests and, then, to compute the long term settlement of the soil beneath the fill. Calibrations were performed to find the model parameters, based on the laboratory consolidation test, first, by assuming the parameters to be those obtained by the tests and, then, to refine the model parameters in such a way as to show the best consistency with experimental data. In view of results directly obtained by experimental data, the modulus of elasticity, as one of the important parameters required for the estimation of the consolidation settlement, was first assumed to be equal to the average value obtained directly (roughly around 7300 kPa, during the course of significant pressure for the analysis, i.e. between 0 and 500 kPa). However, after making a few analyses, i.e. by changing the modulus of elasticity and comparing the obtained results, the calibrated modulus of elasticity was reasonably found to be 6400 kPa and to be compatible with the averaged load-displacement curve of all consolidation tests. A proper choice for this parameter was found to be very important in the deformation analysis. It was found to be slightly different from the average modulus of elasticity directly found by test data. Figure 2 shows the results, obtained both experimentally (from consolidation tests) and numerically, to find the model parameters for the rest of the study. It can be seen that, except for one test, almost all results obtained experimentally obey the

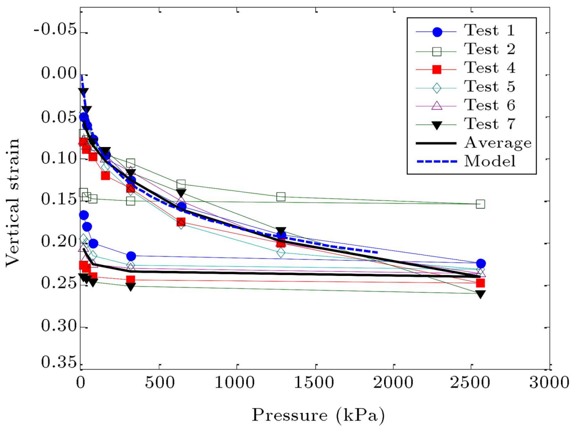

Figure 2. Laboratory consolidation test results along with predictions made by the model.

same trend. Calibration was made in order to capture the trend of the average of all test results, i.e. the bold line in the figure. It is noticeable that the vertical strain, shown on the vertical axis, is, in fact, nothing but simply the ratio of the vertical displacement to the height of the sample at the end of each test. Figure 3 shows the dissipation of the excess pore water pressure in a consolidation test under 320 kPa pressure. Results are plotted for elapsed times of 4 hours, 8 hours and 16 hours. The final deformed shape of the model

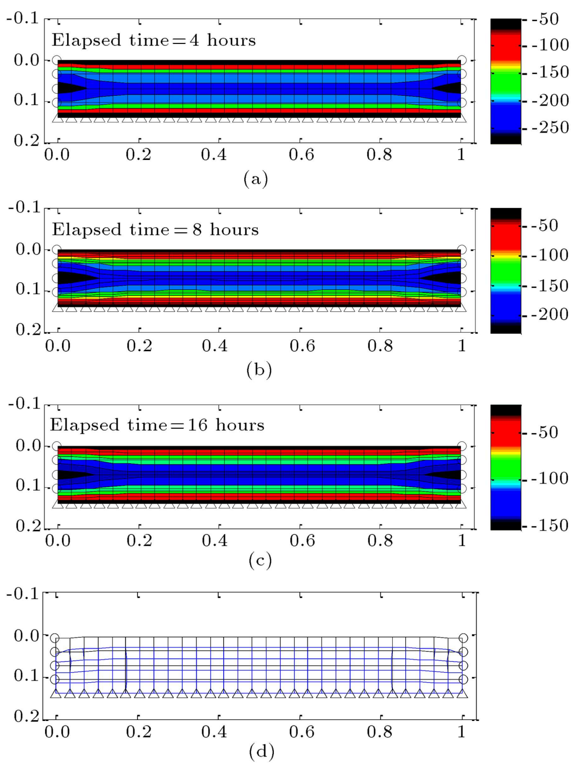

Figure 3. Excess pore water pressure dissipation after (a) 4 hours, (b) 8 hours, and (c) 16 hours along with (d) the deformed mesh at the end of the consolidation test (scaled up 5 times; units are in kPa).

is also presented in the same figure. Eventually, in Figure 4, the isochrones of excess pore water pressure distribution along a sample of the soil in the consolidation test, under 320 kPa pressure, are presented. These isochrones were obtained both analytically, by the closed form solution of the consolidation equation evaluated at four points in the sample, and numerically, by the developed code. Isochrones were computed at 2 hour intervals, normalized to the initial excess pore water pressure, which was equal to 320 kPa, uniformly distributed throughout the sample height.

Further analyses were made to simulate the staged construction loading during the preloading process. It is remarkable that the significant difference between these two methods is the computational time. In the small strain analysis, the stiffness matrix is once computed and assembled. However, in the large strain analysis, it should be recomputed at each increment, which results in a quite longer computation. The time efficiency can be increased by reducing the number of elements in the model, i.e. based on the required precision, an optimum number of elements can be used, which differs from problem to problem. To optimize computational effort, a total number of 38 loading steps were taken, i.e. displacements were computed at every two days from the start of the loading. A total number of 48 sub-increments were used to accurately model dissipation of the excess pore water pressure during each loading step. It should be noted that for a smaller load increment, i.e. larger number of loading steps, computational effort was found to be relatively longer, while the change in the results was slight and insignificant.

Figure 5 shows an outline of the model, the geometry of the problem and boundary conditions. Using a standard boundary condition for such problems,

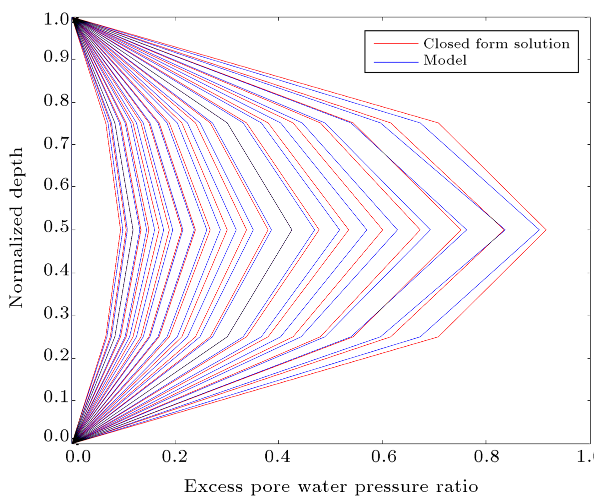

Figure 4. Excess pore water pressure isochrones for a typical consolidation test performed under 320 kPa pressure.

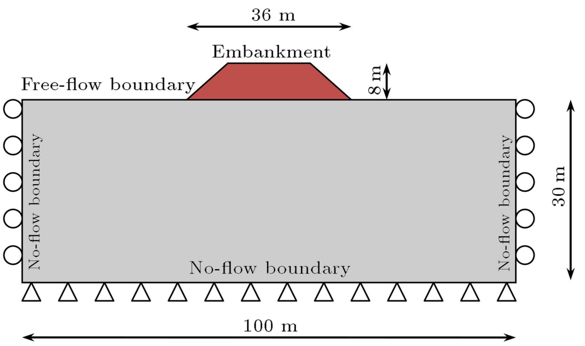

Figure 5. Geometry and boundary conditions of the model.

the lateral displacements at right and left sides were restrained. Moreover, the bottom of the model was completely restrained against both vertical and lateral displacements. The boundary conditions for transient fluid flow consist of no flow boundaries at vertical sides and in the bottom of the model, whereas the uppermost boundary was assumed to be held at zero excess pore water pressure (free flow boundary).

Figures 6-9 show the model predictions for elapsed times of 8 days (embankment height equal to 2 m), 18 days (embankment height equal to 6 m), 22 days (end of embankment construction) and 60 days (approaching an almost steady state), respectively. In these figures, distribution of the excess pore water pressure, along with the deformed mesh (scaled up 5 times) and velocity fields, is presented. In Figure 10, predicted and measured settlements are plotted. Moreover, the predicted consolidation settlement, computed by the small strain analysis, is plotted on the same graph. It is evident that predictions made by the large strain analysis comply better with measured data, i.e. the trend and final amount of settlement have been better captured.

5. Numerical technique and conventional methods

Methods based on conventional formula have been also widely applied in many projects. Such methods require only the direct use of the results obtained by standard laboratory tests, such as m_v and the unit weight, and no further interpretation of the test results, as well as indirect parameters, is required. When the surcharge pressure spreads over a reasonably wide area, assuming a one-dimensional deformation is not too far from real behavior. However, where the loaded area is quite finite in comparison to the thickness of the consolidating layer, such methods should be subjected to some corrections, since direct use of laboratory consolidation tests is not satisfactory. In addition, lateral deformations cannot be ignored. Therefore, the

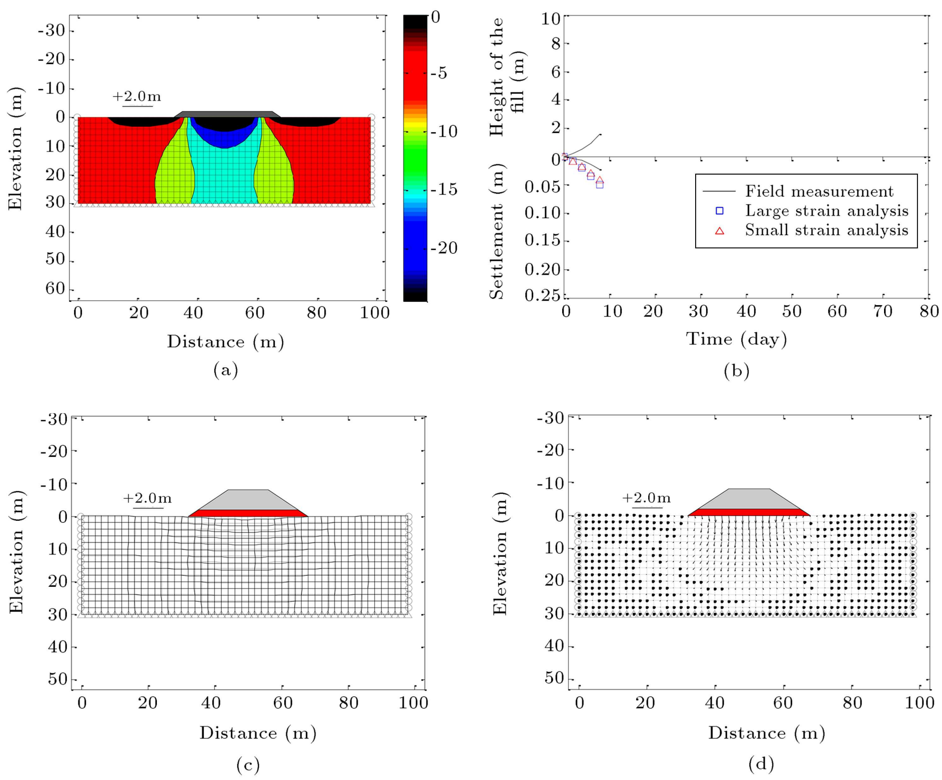

Figure 6. Predicted and measured consolidation settlement after 8 days: (a) Distribution of the excess pore water pressure; (b) height-time-settlement graph; (c) deformed mesh; and (d) displacement increments (velocity) field (scaled up 5 times).

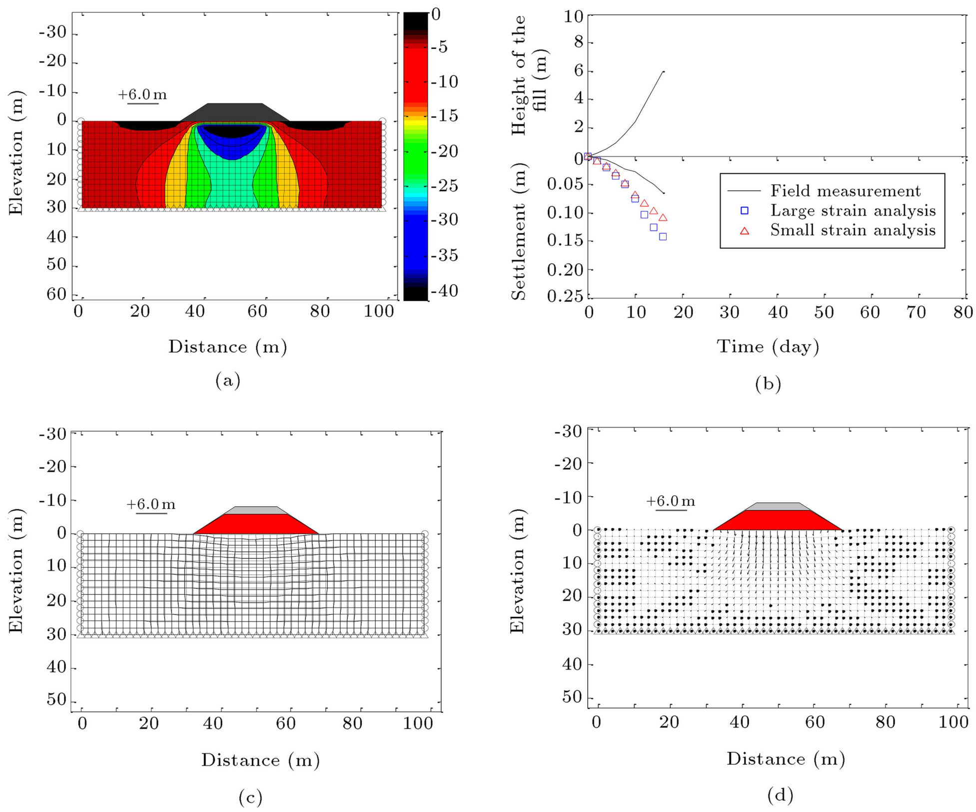

Figure 7. Predicted and measured consolidation settlement after 18 days: (a) Distribution of the excess pore water pressure; (b) height-time-settlement graph; (c) deformed mesh; and (d) displacement increments (velocity) field.

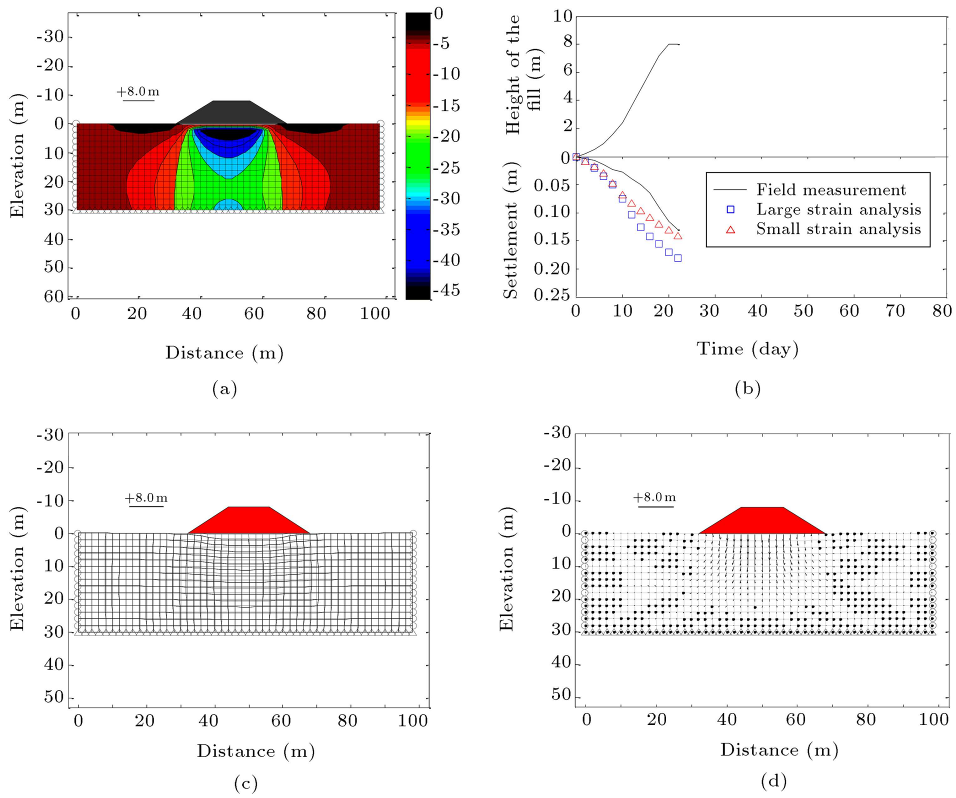

Figure 8. Predicted and measured consolidation settlement after 22 days: (a) Distribution of the excess pore water pressure; (b) height-time-settlement graph; (c) deformed mesh; and (d) displacement increments (velocity) field.

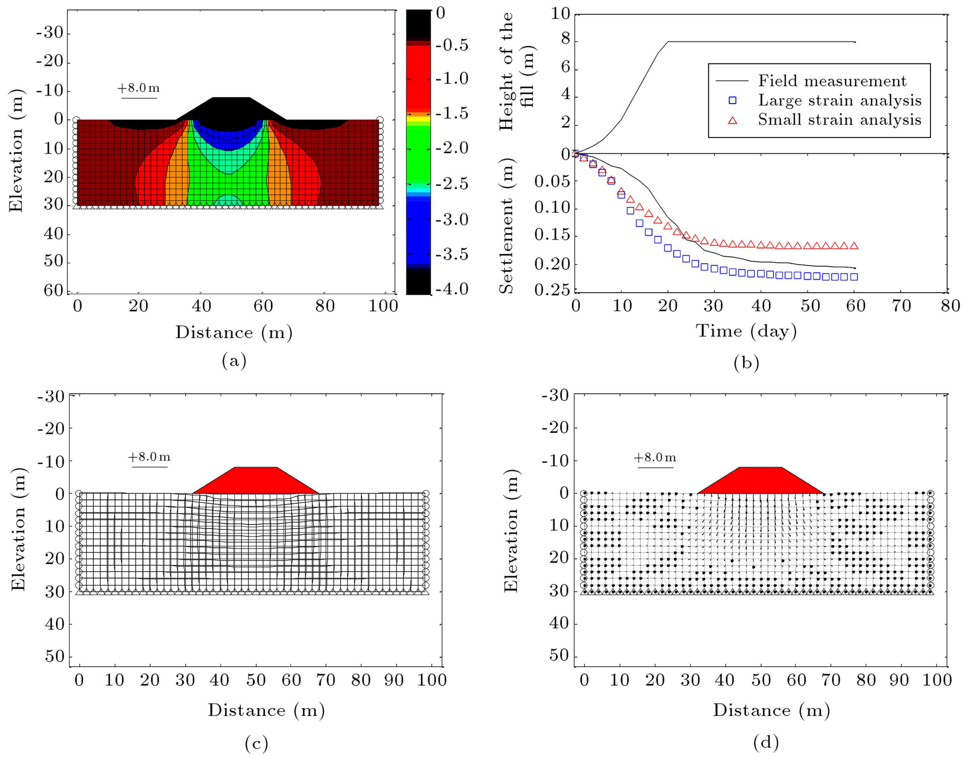

Figure 9. Predicted and measured consolidation settlement after 60 days: (a) Distribution of the excess pore water pressure; (b) height-time-settlement graph; (c) deformed mesh; and (d) displacement increments (velocity) field.

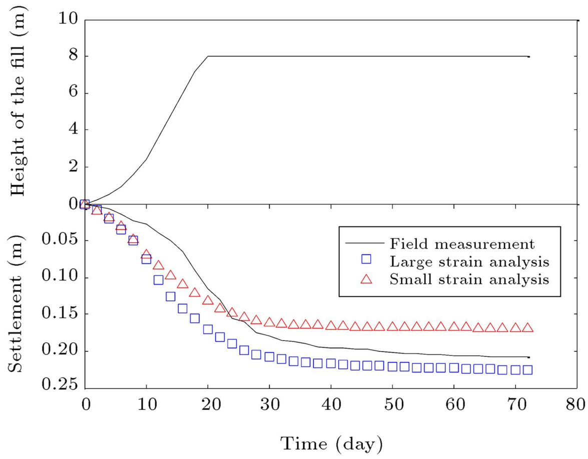

Figure 10. Predicted and measured consolidation settlement after 75 days.

test condition (zero lateral strain) and the site condition (non-zero lateral displacements) will no longer be consistent and, hence, development of excess pore water pressure cannot be directly related to the change in vertical stress only [23,24]. Numerical techniques based on the finite element method, can be always regarded as more precise methods to the same problem, i.e. the analysis of flow, in conjunction with the associated deformation due to the drainage of water, causes volume change in two or three dimensions, since:

i) They consider the two (or three) dimensional water flow;

ii) They consider the lateral deformations.

Although fully 3D methods are often more precise, 2D methods, in particular cases where the physics of the problems allows for plane strain or axi-symmetric simplifications (as in the current study), are precise enough as well.

As a simple alternative, it is also possible to consider such inconsistency by the application of a correction factor, suggested by Skempton and Bjerrum (1957) [25]. The Skempton-Bjerrum method expresses the consolidation settlement due to excess pore water pressure build up in the soil mass by the following equations:

$$S_c = \mu S_c^{oed}, \tag{34}$$

$$S_c^{oed} = \int_{z_1}^{z_1+h} m_v \Delta\sigma_z dz, \tag{35}$$

where S_c is the consolidation settlement, S_c^{oed} is the consolidation settlement based on the laboratory test results, $\Delta\sigma_z$ is the effective vertical stress increment, μ is a correction factor depending on the geometry of the loaded area, and the excess pore water pressure coefficient, A, responsible for the development of the

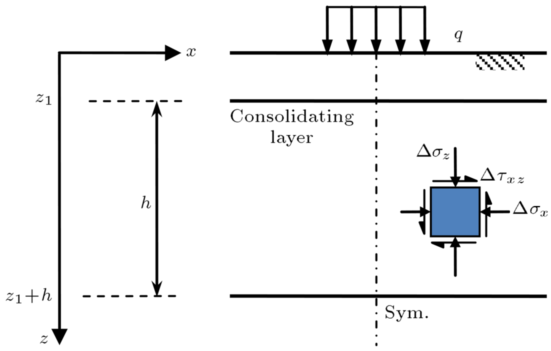

Figure 11. Geometry and stress definitions in consolidation analysis with conventional method.

excess pore water pressure in a consolidation process, z_1 is the depth of the consolidating layer and h is the thickness of the consolidating layer. These parameters are shown in Figure 11.

Theoretically, the correction factor, μ, is defined as follows:

$$\mu = A(1 - A)\alpha, \tag{36}$$

$$\alpha = \frac{\int_{z_1}^{z_1+h} \Delta\sigma_3 dz}{\int_{z_1}^{z_1+h} \Delta\sigma_1 dz}. \tag{37}$$

In these equations, h is the thickness of the consolidating layer, $\Delta\sigma_3$ and $\Delta\sigma_1$ are changes in the minor and major effective principal stresses due to application of the surcharge pressure, respectively. A careful calculation of the settlement was also made to compare the results obtained by the finite element procedure and the conventional method. One of the most accurate approaches is to divide the soil layer into several sublayers. Then, the change in both vertical and lateral stresses can be found by expressions developed for uniformly distributed load and ramp loads (linearly increasing), which are represented in Appendix B.

By making use of 30 sublayers, each 1.0 m thick, and application of the Skempton-Bjerrum method, the total amount of settlement was approximated for different values of m_v. Results were then compared to those obtained by the finite element method and shown in a comparative way in Table 2. It is evident that the values computed by the conventional approach are all overestimated, although the Skempton-Bjerrum correction makes the results much more logical. Although it requires a number of further analyses for different situations, it can be concluded that predictions based on conventional methods (one-dimensional analysis) may often lead to an overestimation of settlement. In contrast, the numerical techniques give better approximations due to better computation of the stress and strain field in a more complete two (or three) dimensional analysis. Moreover, it is evident from the results that predictions based on small and large strain assumptions differ only about 30%. Although this difference is not insignificant, the use of the large strain analysis seems to be more conservative, as it slightly overestimates the amount of final consolidation settlement. Therefore, if the computational effort is not a matter of concern, the large strain finite element formulation, which can be easily calibrated with standard experimental data, and its independence of a complicated elasto-plastic soil model, sounds to be practically more reliable for this important project.

In the same table, the computational times are also presented for both small and large strain analyses. It is remarkable that the computational times correspond to two successive computational steps, i.e. a complete round of stiffness matrix computation and its global assemblage. At first sight, it can be observed that there is an insignificant difference (around 5%) between these two methods. Although, as the mesh size increases, this difference may be added up and accumulated, causing larger computational time effort for large rather than small strain analysis, use of multi-core high-speed processors can well cover this deficiency.

6. Conclusions

Prediction of the consolidation settlement of clay has been found to be a challenging task regarding the nonlinear behavior of soil when it is subjected to applied loads. This nonlinearity can be originated from the elasto-plastic behavior of clay after it reaches the yield surface, i.e. it passes the limits corresponding to the over-consolidation pressure. However, the consolidation equation of Terzaghi (1943) has been practically accepted, since it does not depend on any assumptions based on plasticity theory. It simply assumes that the soil obeys an elastic behavior based on small strain theory, defined over the range of the applied load. Then, the flow and deformation equations are combined to form the uncoupled consolidation equation. Under some special conditions, i.e. in projects of higher importance, when only the consolidation test results are available, this theory may be insufficient to give rise to proper predictions. In such cases, a coupled analysis may provide better results. However, there is another very important source of nonlinear response to applied loads, which cannot be considered by either of these methods. Nonlinearity, owing to large deformations, will not be well captured by the methods based on small strain theory. Therefore, in cases where only standard laboratory test results are available, a better estimate of the consolidation settlement can be achieved by making use of the large deformation analysis. The updated Lagrangian large deformation formulation was

Table 2. Estimated amount of settlement by different methods.

Method in settlement computation	**Coefficient of volume compressibility, m_v**			**Computational time* (sec.)**	**Remarks**
	Minimum 6.5e-5	**Maximum 2.0e-4**	**Average 1.1e-5**		
Consolidation settlement, S_c^{oed}	0.34	0.98	0.54	-	
Corrected consolidation settlement, S_c (Skepmton-Bjerrum method)	0.24	0.71	0.39	-	
Small strain finite element analysis	0.17	0.17	0.17	7.3280	Mesh size: $16\times 50=800$ nodes, Stiffness matrix: 1600×1600
Large strain finite element analysis	0.23	0.23	0.23	7.7180	Mesh size: $16\times 50=800$ nodes, Stiffness matrix: 1600×1600
Measured value	0.21	0.21	0.21	-	

* System (hardware) properties: CPU Intel® (Pentium®) at 3.42GHz, Ram DDRII 2.00GB, HDD: 34.5GB available space on the drive, Software: Windows XP, MATLAB 2011b.

employed, along with flow equations, to solve the coupled consolidation equations.

A case study in Iran was investigated and the consolidation settlement was computed using different methods comprising the finite element techniques and conventional approaches. Some simplifying assumptions were made and model calibrations were performed based on standard laboratory consolidation tests. Results indicated that better results will be obtained if the geometrical nonlinearity is taken into account. Although the results based on the small strain analysis showed smaller settlements in comparison to measured data, due to the complexity and even nonlinearity of the system of equations, they cannot be generalized. Finally, application of the conventional method was found to result in an overestimation of the settlement, even in cases where the minimum value of the volume compressibility index was assumed. As a conclusion, where only the standard laboratory test results are available, and in absence of a nonlinear elasto-plastic constitutive model, the large deformation finite element formulation, calibrated for standard laboratory test results, can estimate both the amount and rate of the consolidation settlement with reasonably good accuracy. Therefore, there are two advantages:

i) The large strain analyses can be calibrated with standard laboratory test results (independency to complicated elasto-plastic models, since it does not involve material nonlinearity);

ii) Results obtained by the large strain analysis are often more reliable, as the small strain analysis may underestimate the amount of consolidation settlement, which may be unsafe in practice.

Acknowledgement

The database of this research project was provided by the Department of Structural and Civil Engineering at the Hampa Energy Engineering and Design Company (HEDCO), Shiraz, Iran, with which the author cooperated in many projects during 2009 and 2010. The author especially appreciates the significant assistance given by all contributors from that company, in particular Mr. Hassan Sedighi, department head, as well as the managing director, deputies, and all respected personnel.

References

1. Terzaghi, K., *Theoretical Soil Mechanics*, John-Wiley and Sons Inc., NY (1943).
2. Biot, M.A. "General theory of three dimensional consolidation", *J. App. Phys.*, **12**, pp. 155-164 (1941).
3. Biot, M.A. "Theory of elasticity and consolidation for a porous anisotropic solid", *J. App. Phys.*, **26**(2), pp. 182-185 (1955).
4. Mikasa, M. "The consolidation of soft clay - a new consolidation theory and its application", Kajima Institution, Tokyo (1963). (In Japanese).
5. Gibson, R.G., England, G.L. and Hussey, M.J.L. "The theory of one-dimensional consolidation of saturated clays", Géotechnique, **17**(3), pp. 261-273 (1967).
6. Gibson, R.G., Schiffman, R.L. and Cargill, K.W. "The theory of one-dimensional consolidation of saturated clays II. Finite nonlinear consolidation of thick homogeneous clays", *Can. Geotech. J.*, (18), pp. 280-293 (1981).
7. Huerta, A. and Rodriguez, A. "Numerical analysis of nonlinear large strain consolidation and filling", *Computers and Structures*, **44**(1-2), pp. 357-365 (1992).

8. Desai, C.S. and Johnson, L.D. "Evaluation of two finite element formulations for one-dimensional consolidation", *Computers and Structures*, **2**, pp. 469-486 (1972).

9. Johnson, C. "A finite element method for consolidation of clay", *Comp. Meth. Appl. Mech. Eng.*, **16**, pp. 178-184 (1978).

10. Duncan, J.M. and Schaefer, V.R. "Finite element analysis of embankments", *Computers and Geotechnics*, **6**(2), pp. 77-93 (1988).

11. Borja, R.I., Tamagntm, C. and Alarcón, E. "Elastoplastic consolidation at finite strain. Part 2: Finite element implementation and numerical examples", *Comp. Meth. Appl. Mech. Eng.*, **159**, pp. 103-122 (1998).

12. Kelln, C., Sharma, J., Hughes, D. and Graham, J. "Finite element analysis of an embankment on a soft estuarine deposit using an elastic-viscoplastic soil model", *Can. Geotech. J.*, **46**(3), pp. 357-368 (2009).

13. Huang, J. and Griffiths, D.V. "One-dimensional consolidation theories for layered soil and coupled and uncoupled solutions by the finite-element method", *Géotechnique*, **60**(9), pp. 709-713 (2010).

14. Samimi, S. and Pak, A. "Three-dimensional simulation of fully coupled hydro-mechanical behavior of saturated porous media using Element Free Galerkin (EFG) method", *Computers and Geotechnics*, **46**, pp. 75-83 (2012).

15. Bathe, K.-J., *Finite Element Procedures*, Prentice-Hall, New Delhi, India (1996).

16. Bonet, J. and Wood, R.D., *Nonlinear Continuum Mechanics for Finite Element Analysis*, Cambridge University Press (1997).

17. Borja, R.I. and Alarcón, E. "A mathematical framework for finite strain elastoplastic consolidation. Part 1: Balance laws, variational formulation, and linearization", *Comp. Meth. Appl. Mech. Eng.*, **122**, pp. 145-171 (1995).

18. Potts, D.M. and Zdrakovic, L., *Finite Element Analysis in Geotechnical Engineering: Theory*, Thomas Telford, London, UK (1999).

19. Reddy, J.N., *An Introduction to Nonlinear Finite Element Analysis*, Oxford University Press, Oxford, UK (2004).

20. Zienkiewicz, O.C. and Taylor, R.L., *The Finite Element Method for Solid and Structural Mechanics*, 5th Ed., Elsevier (2005).

21. Itskov, M., *Tensor Algebra and Tensor Analysis for Engineers with Applications to Continuum Mechanics*, 2nd Ed., Springer (2009).

22. Booker, J.R. and Small, J.C. "An investigation of the stability of the numerical solutions of Biot's equations of consolidation", *Int. J. Solids Struct.*, **11**(7-8), pp. 907-917 (1975).

23. Craig, R.F., *Soil Mechanics*, 4th Ed., Chapman and Hall (1987).

24. Holtz, R.D. and Kovacs, W.D., *An Introduction to Geotechnical Engineering*, Prentice Hall (1981).

25. Skempton, A.W. and Bjerrum, L. "A contribution to the settlement analysis of foundations on clay", *Géotechnique*, **7**(4), pp. 168-178 (1957).

Appendix A

Required equations for the updated Lagrangian finite element formulation

The following equations are used in the updated Lagrangian large deformation finite element formulation for two-dimensional problems found in advanced texts ([15,19] among others):

$$\mathbf{B_L} = \begin{bmatrix} \frac{\partial \phi_1}{\partial x} & 0 & \cdots & 0 \\ 0 & \frac{\partial \phi_1}{\partial y} & \cdots & \frac{\partial \phi_n}{\partial y} \\ \frac{\partial \phi_1}{\partial y} & \frac{\partial \phi_1}{\partial x} & \cdots & \frac{\partial \phi_n}{\partial x} \end{bmatrix}, \tag{A.1}$$

$$\mathbf{B_{NL}} = \begin{bmatrix} \frac{\partial \phi_1}{\partial x} & 0 & \cdots & 0 \\ \frac{\partial \phi_1}{\partial y} & 0 & \cdots & 0 \\ 0 & \frac{\partial \phi_1}{\partial x} & \cdots & \frac{\partial \phi_n}{\partial x} \\ 0 & \frac{\partial \phi_1}{\partial y} & \cdots & \frac{\partial \phi_n}{\partial y} \end{bmatrix}, \tag{A.2}$$

$$\mathbf{{}^1\boldsymbol{\sigma}} = \begin{bmatrix} {}^1\sigma_{xx} & {}^1\sigma_{xy} & 0 & 0 \\ {}^1\sigma_{xy} & {}^1\sigma_{yy} & 0 & 0 \\ 0 & 0 & {}^1\sigma_{xx} & {}^1\sigma_{xy} \\ 0 & 0 & {}^1\sigma_{xy} & {}^1\sigma_{yy} \end{bmatrix}, \tag{A.3}$$

$$\mathbf{{}^1\underline{\boldsymbol{\sigma}}} = \begin{bmatrix} {}^1\sigma_{xx} \\ {}^1\sigma_{yy} \\ {}^1\sigma_{xy} \end{bmatrix}, \tag{A.4}$$

$$\mathbf{{}^1\underline{\boldsymbol{\sigma}}} = \mathbf{D_1^1}\underline{\boldsymbol{\varepsilon}}, \tag{A.5}$$

$${}^1_1\underline{\boldsymbol{\varepsilon}} = \begin{bmatrix} {}^1_1\varepsilon_{xx} \\ {}^1_1\varepsilon_{yy} \\ 2{}^1_1\varepsilon_{xy} \end{bmatrix} = \begin{bmatrix} \frac{\partial u_x}{\partial x} - \frac{1}{2}\left(\left(\frac{\partial u_x}{\partial x}\right)^2 + \left(\frac{\partial u_y}{\partial x}\right)^2 \right) \\ \frac{\partial u_y}{\partial y} - \frac{1}{2}\left(\left(\frac{\partial u_x}{\partial y}\right)^2 + \left(\frac{\partial u_y}{\partial y}\right)^2 \right) \\ \frac{\partial u_x}{\partial y} + \frac{\partial u_y}{\partial x} - \frac{1}{2}\left(\frac{\partial u_x}{\partial x}\frac{\partial u_x}{\partial y} + \frac{\partial u_y}{\partial x}\frac{\partial u_y}{\partial y} \right) \end{bmatrix}. \tag{A.6}$$

Appendix B

Conventional consolidation settlement computation

The required equations for the horizontal and vertical stress changes in depth are as follows. Parameters are shown in Figure B1 (redrawn based on Craig,

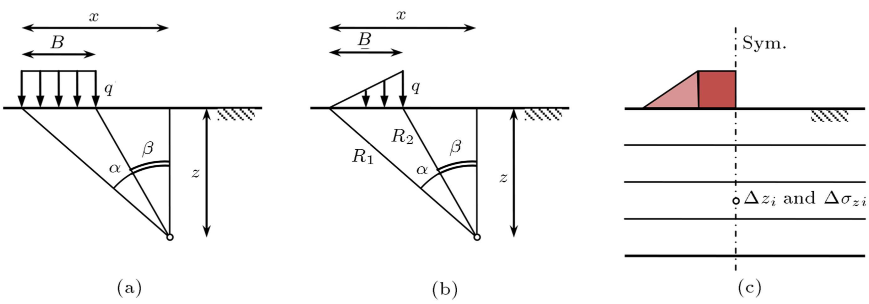

Figure B1. Parameters involved in vertical and lateral stress change due to: (a) uniformly distributed load, (b) ramp load, and (c) discretization of the consolidating layer in conventional approach.

1987 [23]).

For uniformly distributed load:

$$\Delta\sigma_x = \frac{q}{\pi}[\alpha - \sin\alpha\cos(\alpha + 2\beta)], \tag{B.1}$$

$$\Delta\sigma_z = \frac{q}{\pi}[\alpha + \sin\alpha\cos(\alpha + 2\beta)], \tag{B.2}$$

For ramp (linearly increasing) load:

$$\Delta\sigma_x = \frac{q}{\pi}\left[\frac{x}{B}\alpha - \frac{z}{B}\ln\frac{R_1^2}{R_2^2} + 0.5\sin 2\beta\right], \tag{B.3}$$

$$\Delta\sigma_z = \frac{q}{\pi}\left[\frac{x}{B}\alpha - 0.5\sin 2\beta\right]. \tag{B.4}$$

The increments of the settlement in each layer and the final settlement were approximated, numerically, as follows:

$$S_c^{oed} = \int_{z_1}^{z_2+h} m_v \Delta\sigma_z dz \cong \sum_{i=1}^{n} m_v \Delta\sigma_{zi}\Delta z_i. \tag{B.5}$$

It is remarkable that $\Delta\sigma_x$ and $\Delta\sigma_z$ reduce to $\Delta\sigma_3$ and $\Delta\sigma_1$, respectively, along the centerline of the loaded area (if it is symmetric).

Biography

Mehdi Veiskarami was born in Tehran, Iran. He received BS and MS degrees in Civil Engineering and Geotechnical Engineering from the University of Guilan, Iran, in 2003 and 2005, respectively, and his PhD degree in Geomechanics from Shiraz University, Iran. under supervision of Prof. A. Ghahramani and Prof. M. Jahanandish, in May 26, 2010. He is currently Assistant Professor at the University of Guilan, Iran. Dr. Veiskarami has published several papers, mainly in the area of computational geomechanics and soil plasticity, and has reasonable engineering experience in large scale projects, in particular oil, gas and petrochemical industries development.